

Dual Divalent Cation Requirement of the MutT dGTPase

KINETIC AND MAGNETIC RESONANCE STUDIES OF THE METAL AND SUBSTRATE COMPLEXES*

(Received for publication, July 8, 1993, and in revised form, September 28, 1993)

David N. Frick^{‡§}, David J. Weber^{||}, Joel R. Gillespie[¶], Maurice J. Bessman[‡], and Albert S. Mildvan^{¶**}

From the [‡]Department of Biology, The Johns Hopkins University, Baltimore, Maryland 21218 and the [¶]Department of Biological Chemistry, The Johns Hopkins School of Medicine, Baltimore, Maryland 21205

Kinetic analyses of both the Mn²⁺- and Mg²⁺-activated hydrolysis of dGTP by MutT show the requirement for two divalent cations. Whereas Mn²⁺ supports a 20-fold lower *k*_{cat} (0.19 s⁻¹) than Mg²⁺ (4.0 s⁻¹), the *K*_m of Mn²⁺·dGTP (6.3 μM) is 45-fold lower than that of Mg²⁺·dGTP (284 μM). Adenosine 5'-(α,β-methylenetriphosphate) (AMPCPP) is a linear competitive inhibitor with respect to dGTP with a *K*_i for Mn²⁺·AMPCPP (42 μM) which is 57-fold lower than the *K*_i of Mg²⁺·AMPCPP (2.4 mM). Such tightening suggests that a metal-bridge E·M²⁺·NTP·M²⁺ complex is the catalytically active species. The 12 dissociation constants describing the quaternary MutT·M²⁺·AMPCPP·M²⁺ complex were evaluated for both Mn²⁺ and Mg²⁺, using EPR and NMR methods. MutT binds a single Mn²⁺ with a *K*_d of 130 ± 40 μM in reasonable agreement with the kinetically determined activator constant of Mn²⁺ of 230 ± 72 μM. The MutT·AMPCPP complex binds two Mn²⁺ ions, the weaker of which has a *K*_d of 16 ± 2 μM in agreement with the kinetically determined *K*_{Mn²⁺} of 26 ± 10 μM. MutT·Mn²⁺ binds Mn²⁺·AMPCPP with *K*_d of 16 ± 4 μM, whereas MutT alone binds Mn²⁺·AMPCPP with a *K*_d of 135 ± 30 μM. The 17-fold enhanced paramagnetic effect of Mn²⁺ on the longitudinal relaxation rate of water protons found with the binary MutT·Mn²⁺ complex decreases to 4.7-fold upon binding of AMPCPP and to 8.7-fold upon binding of Mn²⁺·AMPCPP, further supporting a metal-bridge MutT·M²⁺·NTP·M²⁺ complex. By competition with Mn²⁺ MutT binds Mg²⁺ at one site with a *K*_d of 7.5 mM, and MutT·AMPCPP binds Mg²⁺ at two sites, the weaker of which has a *K*_d of 0.9 mM. These values are comparable to the kinetically determined *K*_{Mg²⁺} of 15 ± 7 mM and *K*_{Mg²⁺} of 1.7 ± 0.7 mM, respectively. Studies with the racemic, substitution-inert β,γ-bidentate tetraamminecobalt (III)-β,γ-phosphate-ATP (Co³⁺(NH₃)₄ATP) complex show that MutT slowly hydrolyzes only the Λ stereoisomer but requires Mg²⁺ or Mn²⁺ to do so, confirming a dual metal ion requirement.

Although *mutT* was the first mutator gene discovered in *Escherichia coli* (Treffers *et al.*, 1954), relatively little is known

* This work supported in part by National Institutes of Health Grant DK28616 (to A. S. M.) and Grant GM18649 (to M. J. B.). The costs of publication of this article were defrayed in part by the payment of page charges. This article must therefore be hereby marked "advertisement" in accordance with 18 U.S.C. Section 1734 solely to indicate this fact.

§ Supported by National Institutes of Health Training Grant 5-T32-GM07231.

|| Present address: Dept. of Biological Chemistry, University of Maryland School of Medicine, 108 N. Greene St., Baltimore, MD 21201.

** To whom correspondence should be addressed: Dept. of Biological Chemistry, The Johns Hopkins School of Medicine, 725 N. Wolfe St., Baltimore, MD 21205. Tel.: 410-955-2038; Fax: 410-955-5759.

at the molecular level about why a defective *mutT* gene results in a thousand-fold increase in a single class of DNA base pair substitution, an A:T to C:G transversion (Yanofsky *et al.*, 1966; Fowler *et al.*, 1992). To date, the only enzymatic activity demonstrated for the MutT protein is a nucleoside triphosphatase that hydrolyzes all canonical nucleoside triphosphates (NTPs)¹ with a preference for deoxyguanosine triphosphate (dGTP) (Bhatnagar and Bessman, 1988; Akiyama *et al.*, 1989; Bhatnagar *et al.*, 1991). This activity is linked to the mutator phenotype (Bhatnagar *et al.*, 1990), and strains that produce MutT protein with low dGTPase activity concomitantly display high mutation rates (Bullions, 1993). Homologs of the *mutT* gene have been isolated in other organisms (Bullions, 1993), and a hydrolase for 8-oxo-dGTP which may be related to the bacterial enzymes has recently been reported in human cells (Mo *et al.*, 1992).

The hydrolysis of dGTP in the MutT-catalyzed reaction occurs through a nucleophilic substitution at the rarely attacked β-phosphorus atom of dGTP to yield dGMP and pyrophosphate (Weber *et al.*, 1992). In biological reactions, substitutions at the α-phosphorus of an NTP to yield pyrophosphate are common. There are currently only six other enzymes, all synthetases, known to catalyze substitution at the β-phosphorus of an NTP, presumably because of the greater electron density at this position (Mildvan, 1970). MutT is the first hydrolase in this small group. This unique chemistry makes physical studies of the MutT enzyme of substantive mechanistic interest.

Like MutT, the six synthetases that catalyze nucleophilic substitution at the β-phosphorus of an NTP all require divalent cations for activity. Phosphoribosylpyrophosphate synthetase (Switzer, 1971; Li *et al.*, 1978; Granot *et al.*, 1980) and phosphoenolpyruvate synthase (Berman and Cohn, 1970) have been shown by both kinetic and metal binding studies to require two divalent cations at the active site. With pyruvate-orthophosphate dikinase (Michaels *et al.*, 1978) and thiamin pyrophosphokinase (Kaziro, 1959) kinetic data suggest a dual divalent cation requirement, since optimal activity is achieved only when the concentration of the divalent cation activator well exceeds the level required to saturate the NTP substrate. Although the metal ion requirements have not been investigated quantitatively for dihydropteridine pyrophosphokinase (Shiota *et al.*, 1969) or for 3-pyrophosphoryl-guanosine diphosphate synthetase (Sy and Lipmann, 1973), the concentrations of Mg²⁺ used in routine assays of these enzymes far exceed the levels required to saturate the NTP. These observations raise the interesting possibility that all enzymes that catalyze nucleophilic substitution at the electron rich β-phosphorus of

¹ The abbreviations used are: NTP(s), nucleoside triphosphate(s); Co³⁺(NH₃)₄ATP, tetraamminecobalt (III)-β,γ-phosphate-ATP; AMPCPP, adenosine 5'-(α,β-methylenetriphosphate); HSQC, heteronuclear single quantum coherence.

NTP may require two divalent cations to do so. The MutT reaction, a relatively simple hydrolysis, rather than a complicated synthetic process, provides a unique opportunity to test this possibility further. The present study demonstrates, by both kinetic and binding studies, that the MutT reaction requires two divalent cations. One metal coordinates the β - and γ -phosphates of the NTP substrate, and the other binds to the enzyme, raising its affinity for the metal-NTP complex. These findings suggest the formation of a kinetically active MutT·M²⁺·NTP·M²⁺ metal-bridge complex. A preliminary abstract of this work has been published (Frick *et al.*, 1993).

EXPERIMENTAL PROCEDURES

Materials

Preparation of MutT—The *mutT* gene was subcloned into the plasmid vector pE11b (Novagen) and expressed under control of the T7 promoter in *E. coli* strain HMS174(DE3) (Novagen, Madison, WI). When induced, this system produces 40–50 mg of MutT protein per liter of culture. The soluble MutT enzyme was purified using the method of Bhatnagar and Bessman (1988) except that the final two DEAE-cellulose columns were substituted with a single DEAE-Sepharose fast-flow column at pH 7.5, eluting with 50 mM Tris-Cl, pH 7.5, with a stepwise gradient from 50 to 150 mM NaCl. At this stage, the protein was judged to be more than 98% pure by sodium dodecyl sulfate-gel electrophoresis. The MutT protein was then concentrated by lyophilization and redissolved in 50 mM Tris-Cl, pH 7.5, passed down a Sephadex G-25 column, dialyzed against 1 mM Tris-Cl containing a 0.01% (v/v) suspension of Chelex 100 to remove trace metal contaminants, and again concentrated by lyophilization. The homogeneous MutT protein had a specific activity of 70 ± 5 units/mg under standard assay conditions (Bhatnagar *et al.*, 1991), and a 1% solution of this pure MutT gave an $A_{280}^{1\%} = 22.0$ at pH 7.5.

Preparation of [γ -³²P]dGTP—[γ -³²P]dGTP was prepared by transphosphorylation of dGDP from [γ -³²P]ATP catalyzed by nucleoside-diphosphate kinase (EC 2.7.4.6, Sigma) and purified, as described (Bhatnagar *et al.*, 1991).

Preparation of Co³⁺(NH₃)₄ATP— β , γ -Bidentate Co³⁺(NH₃)₄ATP was prepared and purified and its structure established, as described by Cornelius *et al.* (1988), by ³¹P NMR at 101.25 MHz using a Bruker AM 250 NMR Spectrometer, and by UV-visible absorption spectroscopy from 200 to 650 nm using a Perkin-Elmer-Cetus Instruments Lambda 9 UV/VIS/NIR Spectrophotometer. The Δ stereoisomer was purified from the resulting racemic mixture using yeast hexokinase and glucose to remove the Λ stereoisomer (Cornelius and Cleland, 1978; Li *et al.*, 1978; Cleland and Mildvan, 1979).

Methods

Kinetic Studies—Unless otherwise stated, all kinetic and thermodynamic experiments were done at 23 °C in the presence of 50 mM Tris-Cl, pH 7.5. The concentration of MutT was determined spectrophotometrically using $A_{280}^{1\%} = 22.0$. Concentrations of dGTP were determined using $\epsilon_{252} = 1.37 \times 10^4$ M⁻¹ cm⁻¹, and of AMPCPP using $\epsilon_{259} = 1.54 \times 10^4$ M⁻¹ cm⁻¹.

Kinetic experiments with Mg²⁺- or Mn²⁺-activated MutT were performed by measuring [³²P]pyrophosphate released from [γ -³²P]dGTP as described (Bhatnagar *et al.*, 1991). However, a 50- μ l reaction volume was used, and no bovine serum albumin, glycerol, or EDTA was present in the reaction mixture. Under these conditions, the velocity of the reaction was linear with both time and enzyme concentration, not more than 10% of the substrate was hydrolyzed, and the lowest amount of [³²P]pyrophosphate produced was more than twice that of background levels.

Kinetic studies with Co³⁺(NH₃)₄ATP as substrate were carried out by monitoring changes in the circular dichroism of the racemic complex and independently by the appearance of AMP. CD spectra of Co³⁺(NH₃)₄ATP were collected on an AVIV 60DS spectropolarimeter from 450 to 650 nm by subtracting eight scans of buffer from eight scans of sample. A 2-nm step size was used with a 1-cm path length and 0.5-s integration time. The appearance of AMP was assayed according to the method of Adams (1965) except that 5 mM MgCl₂ was used instead of MgSO₄, 50 mM KCl was added to the reaction mixture, and the coupling enzymes were diluted into 50 mM Tris-Cl, pH 7.5.

Binding Studies—The binding of AMPCPP to the MutT protein in the absence of divalent cations was monitored by the effects of the nucleotide on the chemical shifts of the side chain and backbone NH and ¹⁵N resonances in a series of HSQC experiments (Marion *et al.*, 1989). A

modified Bruker AM 600 NMR spectrometer (Kay *et al.*, 1990; Weber *et al.*, 1992) operating at 600 MHz for protons and at 60.8 MHz for ¹⁵N was used. The enzyme (1.5 mM) enriched with ¹⁵N as described previously (Weber *et al.*, 1993) in a solution containing 5.8 mM Tris-d₁₁-Cl, pH 7.4, 20 mM NaCl, 0.1 mM EDTA, 0.34 mM NaN₃, and 10% D₂O at 32 °C, was titrated with AMPCPP followed by the acquisition of an HSQC spectrum at each point of the titration. The changes in chemical shifts of selected amide proton and ¹⁵N resonances were fit by a hyperbolic titration curve to yield the dissociation constant K_1 of the binary MutT·AMPCPP complex.

The concentration of free Mn²⁺ in a solution containing free and bound Mn²⁺ was determined by electron paramagnetic resonance (EPR) (Cohn and Townsend, 1954) at 9.15 GHz with a Varian E-4 EPR spectrometer. Bound Mn²⁺ was monitored by measurements of the longitudinal relaxation rate ($1/T_1$) of water protons with a Seimco pulsed NMR spectrometer at 24.3 MHz using a 180- π -90° pulse sequence as described previously (Carr and Purcell, 1954; Mildvan and Engle, 1972). The observed enhancement (ϵ^*) of $1/T_1$ by enzyme-bound Mn²⁺ is defined as

$$\epsilon = (1/T_1^* - 1/T_{1,0}) / (1/T_1 - 1/T_{1,0}) \quad (\text{Eq. 1})$$

where $1/T_1$ and $1/T_{1,0}$ equal the longitudinal relaxation rate of water in the presence and absence of Mn²⁺, and $1/T_1^*$ and $1/T_{1,0}^*$ represent the same parameters in the presence of MutT. This observed enhancement (ϵ^*) has been shown to be the weighted average of the enhancements caused by all forms of Mn²⁺. In a solution containing more than one Mn²⁺ species it has been shown that

$$\epsilon^* = \frac{\sum_i [\text{Mn}^{2+}]_i \epsilon_i}{[\text{Mn}^{2+}]_T} \quad (\text{Eq. 2})$$

where $[\text{Mn}^{2+}]_T$ is the total Mn²⁺ present in solution, $[\text{Mn}^{2+}]_i$ is the concentration, and ϵ_i is the enhancement of the i th complex of Mn²⁺ (Mildvan and Cohn, 1963, 1966).

Because the MutT·AMPCPP complex was found to bind two divalent cations, a method similar to that of Armstrong *et al.* (1979) was used to analyze properly the titrations of MutT with metal ions and with AMPCPP. A complete thermodynamic description of the binding of two metal ions (M) and one AMPCPP (A) per molecule of enzyme (E), to form

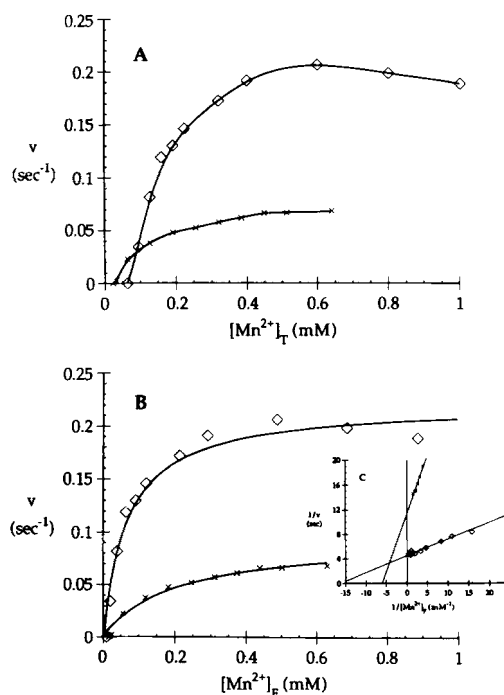


FIG. 1. Mn²⁺ activation of the MutT dGTPase. Panel A, initial velocity of the MutT reaction (mol of dGTP/mol of MutT/s) as a function of total MnCl₂ concentration and at dGTP concentrations of 112 μ M (\diamond) and 10 μ M (\times). Also present was 50 mM Tris-Cl, pH 7.5. Panel B, initial velocity of the MutT reaction as a function of free Mn²⁺ at 112 μ M Mn²⁺·dGTP (\diamond) and 10 μ M Mn²⁺·dGTP (\times). Panel C, double-reciprocal plot of the data in panel B. Data in panels B and C are fit to the equation $v = k_{\text{cat}}[\text{Mn}^{2+}]_F / (K_m^{\text{Mn}^{2+}} + [\text{Mn}^{2+}]_F)$.

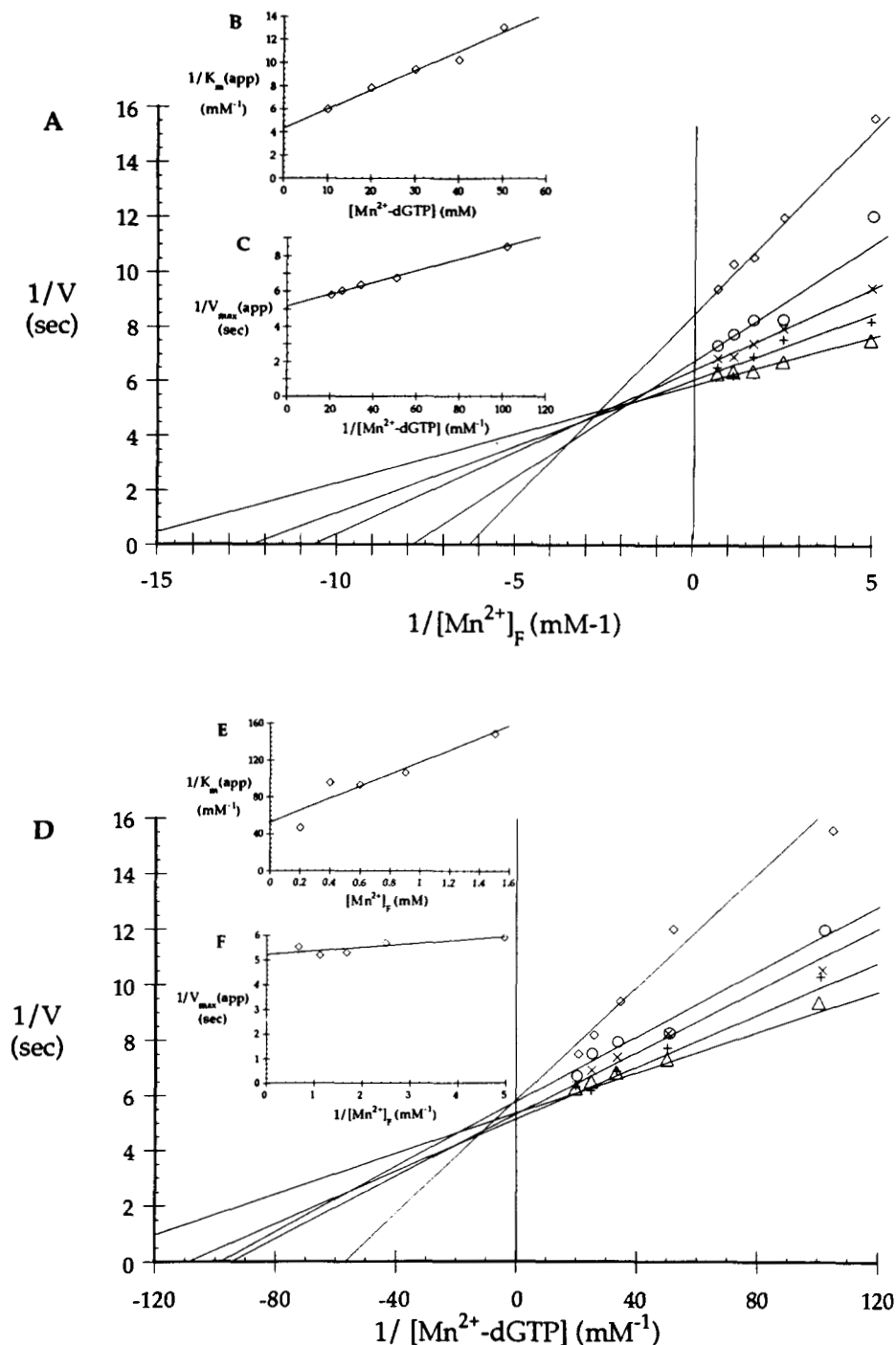


FIG. 2. Kinetics of activation of the MutT dGTPase by Mn^{2+} . Panel A, double-reciprocal plot of initial velocity versus free Mn^{2+} concentration at 10 (\diamond), 20 (\circ), 30 (\times), 40 ($+$), and 50 (Δ) μM Mn^{2+} -dGTP. Also present was 50 mM Tris-Cl, pH 7.5, and 33 nM MutT. Panel B, secondary plot of apparent $1/K_m$ of Mn^{2+} obtained from panel A versus $[Mn^{2+}$ -dGTP] which yields $K_d^{Mn^{2+}}$. Panel C, secondary plot of $1/V_{max(app)}$ at infinite $[Mn^{2+}]$ obtained from panel A against $[Mn^{2+}$ -dGTP], which yields $K_m^{Mn^{2+}$ -dGTP}. Panel D, double-reciprocal plot of initial velocity versus Mn^{2+} -dGTP concentration at 200 (\diamond), 400 (\circ), 600 (\times), 900 ($+$), and 1,500 (Δ) μM Mn^{2+} -dGTP. Panel E, secondary plot of apparent $1/K_m$ of Mn^{2+} -dGTP obtained from panel D versus $[Mn]_F$ which yields $K_s^{Mn^{2+}$ -dGTP}. Panel F, secondary plot of apparent $1/V_{max(app)}$ at infinite $[Mn^{2+}$ -dGTP] obtained from panel D, against $[Mn^{2+}]_F$ which yields $K_m^{Mn^{2+}}$. $[Mn^{2+}]_F$ and $[Mn^{2+}$ -dGTP] were determined using $K_d(Mn^{2+}$ -dGTP) = 10 μM . In panels A and D, data are shown with the lines computed by weighted least squares analysis. In panels B, C, E, and F, lines are computed by least squares analysis.

aquaternary EMAM complex, requires 12 dissociation constants as defined in Table II. From their definitions (Table II),

$$K_1 K_7 = K_2 K_5 = K_3 K_{12} \quad (\text{Eq. 3})$$

$$K_4 K_9 = K_5 K_{11} = K_3 K_6 \quad (\text{Eq. 4})$$

$$K_2 K_4 = K_1 K_{10} = K_3 K_8 \quad (\text{Eq. 5})$$

Hence, only 6 of the 12 dissociation constants are independent. From Equation 2 the following holds.

$$\epsilon^* = [M]_F/[M]_T + ([AM]/[M]_T) \epsilon_b^{AM} + ([EM]/[M]_T) \epsilon_b^{EM} + ([EAM]/[M]_T) \epsilon_t^{EAM} + ([EMA]/[M]_T) \epsilon_t^{EMA} + 2([EMAM]/[M]_T) \epsilon_q \quad (\text{Eq. 6})$$

Iterative computer analysis was used to fit proton relaxation rate titration data to Equation 6 using concentrations determined from the

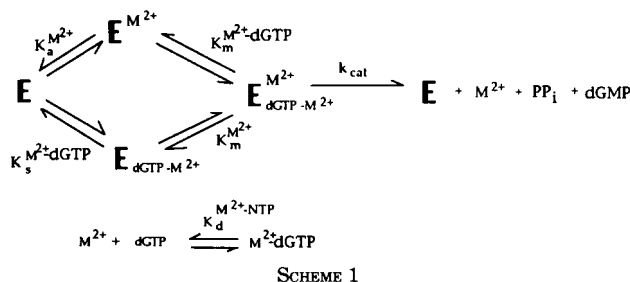
12 dissociation constants. The independently measured parameters used in this analysis were the five dissociation constants K_1, K_2, K_3, K_{10} , and K_{11} , and the two enhancement factors ϵ_b^{EM} and ϵ_b^{AM} . Also known were $[E]_T, [M]_T, [A]_T$, and the observed enhancement ϵ^* at each titration point. The parameters, which were searched by computer, included one dissociation constant (K_6) and two enhancement factors (ϵ_a and ϵ_i). The interrelationships of Equations 3–5 were then used to evaluate the remaining dissociation constants. The dissociation constants for the corresponding Mg^{2+} complexes were determined by competition studies with Mn^{2+} , monitoring the free Mn^{2+} by EPR and the bound Mn^{2+} by ϵ^* , the observed enhancement factor.

RESULTS

Kinetic Studies

Manganese-activated dGTPase—The reaction velocity of an enzyme-catalyzed reaction as a function of the total concentration of a metal activator at constant substrate concentration usually shows a hyperbolic dependence (Dixon and Webb, 1964). However, when MutT is titrated with a metal activator, no reaction is detected until the metal concentration exceeds that of the nucleotide substrate. Fig. 1A shows two such titrations with Mn^{2+} at two different concentrations of dGTP. This effect is explained by the tight dissociation constant for metal nucleotide complexes ($10 \mu M$ for $Mn^{2+} \cdot ATP$) and similar NTPs (Dawson *et al.*, 1986). Fig. 1B shows that, if such a constant is used to calculate the amount of free metal, thereby treating $Mn^{2+} \cdot dGTP$ as the true substrate, the reaction velocity is hyperbolically dependent on the free metal concentration. Such a curve yields a $K_{m(app)}$ and $V_{max(app)}$ for a metal activator at specific metal-NTP concentrations (Fig. 1C).

By varying both metal and substrate concentrations and measuring the initial reaction velocity (Fig. 2), five kinetic parameters can be determined for metal-activated enzymes as defined in Scheme 1. The kinetic data in this study are fit to Scheme 1 using the general rate equation of Dixon and Webb (1964). Fig. 2A shows the dependence of $1/v$ on $1/[Mn^{2+}]_F$ at



different concentrations of $Mn^{2+} \cdot dGTP$. The data are fit using least squares analysis weighted to the free metal concentrations. The extrapolation of a linear plot of $1/K_{m(app)}$ of M^{2+} versus substrate concentration to zero substrate (Fig. 2B) (Serpensu *et al.*, 1986) reveals a $K_a^{Mn^{2+}}$ of $230 \pm 72 \mu M$. The K_m of $Mn^{2+} \cdot dGTP$ at infinite metal concentration $K_m^{Mn^{2+} \cdot dGTP}$ is determined to be $6.3 \pm 0.5 \mu M$ from a secondary plot of $1/V_{max(app)}$ versus $1/[Mn^{2+} \cdot dGTP]$ (Fig. 2C).

The same data, when plotted in the form $1/v$ versus $1/[Mn^{2+} \cdot dGTP]$ at varying levels of Mn^{2+} , can be used to determine the other kinetic constants in Scheme 1 (Fig. 2D). $K_s^{M^{2+} \cdot dGTP}$ for a metal-activated enzyme reaction can be determined to be $22 \pm 13 \mu M$ by extrapolation of $K_{m(app)}(Mn^{2+} \cdot dGTP)$ to zero Mn^{2+} (Fig. 2E). $K_m^{Mn^{2+}}$ is found from Fig. 2F to be $26 \pm 10 \mu M$. Secondary plots of Fig. 2, C and F, both yield the same k_{cat} value for the reaction at infinite metal and infinite substrate of $0.19 \pm 0.01 s^{-1}$ (Table I).

Magnesium-activated dGTPase—Fig. 3 shows that Mg^{2+} activates MutT in a manner similar to Mn^{2+} . A sigmoidal velocity dependence on total $[Mg^{2+}]$ (Fig. 3A) becomes hyperbolic in terms of free $[Mg^{2+}]$ (Fig. 3B) when a $50 \mu M$ binding constant for $Mg^{2+} \cdot dGTP$ (Dawson *et al.*, 1986) is used. A double-reciprocal plot (Fig. 3C) yields an intersecting pattern of lines at different substrate concentrations. In a more detailed study (not shown) all of the constants in Scheme 1 were determined for Mg^{2+} . The concentration of MutT was again $33 nM$, the $[Mg^{2+} \cdot dGTP]$ was varied from 200 to 1,000 μM , and the $[Mg^{2+}]_F$ varied from 1,000 to 12,000 μM .

The resulting kinetic parameters are compared with those obtained with Mn^{2+} in Table I. The values of k_{cat} show that Mn^{2+} supports 20-fold less activity than Mg^{2+} . However, the $K_a^{M^{2+}}$, $K_m^{M^{2+}}$, $K_s^{M^{2+} \cdot dGTP}$, and $K_m^{M^{2+} \cdot GTP}$ are each tightened 45–568-fold with Mn^{2+} , resulting in similar catalytic efficiencies (k_{cat}/K_m) for both Mn^{2+} - and Mg^{2+} -activated MutT dGTPase. The apparent affinity of the enzyme for $Mg^{2+} \cdot dGTP$ is highly dependent on the presence of the second metal ion, as seen by the 44-fold tighter $K_m^{Mg^{2+} \cdot dGTP}$ ($284 \mu M$) when compared with the $K_s^{Mg^{2+} \cdot dGTP}$ ($12.5 mM$). A smaller 3.5-fold tightening effect of the same type is found with Mn^{2+} -activated MutT (Table I).

Inhibition by AMP CPP—To probe the thermodynamics of substrate binding to MutT, a nonhydrolyzable substrate analog was required. Fig. 4 shows the kinetics of inhibition of AMP CPP using either Mn^{2+} or Mg^{2+} as the activator. Since the data in Figs. 1–3 show that the rate of reaction is highly dependent on the concentration of free metal, great care was taken to carry out such competition experiments under conditions of

TABLE I
Comparison of kinetic constants with appropriate dissociation constants of metal and nucleotide complexes of MutT

	Kinetic constants						
	$K_a^{M^{2+}}$	$K_m^{M^{2+}}$	$K_s^{M^{2+} \cdot dGTP}$	$K_m^{M^{2+} \cdot dGTP}$	$K_i^{M^{2+} \cdot AMP CPP}$	$K_d^{M^{2+} \cdot dGTP}$	k_{cat}
	μM						s^{-1}
Mn^{2+}	230 ± 72	26 ± 10	22 ± 13	6.3 ± 0.5	42 ± 10	10^a	0.19 ± 0.01
Mg^{2+}	$14,600 \pm 7,000$	$1,710 \pm 660$	$12,500 \pm 6,200$	284 ± 75	$2,400 \pm 500$	50^a	3.96 ± 0.06
	Dissociation constants						
	K_2^{E-M}	K_{11}^{E-M-AM}	K_{12}^{E-AM}	K_6^{E-AM}	$\langle K_6, K_{12} \rangle^b$	K_3^{A-M}	
	μM						
Mn^{2+}	130 ± 40^c	16.2 ± 2.0^d	135 ± 30^e	16.4 ± 4.2^e	29.4 ± 7.4	12 ± 5^c	
Mg^{2+}	$7,500 \pm 1,200^f$	932 ± 100^f	$2,400 \pm 1,500^g$	284 ± 220^g	$1,300 \pm 900$	50 ± 20^a	

^a From Dawson *et al.* (1986).

^b Weighted average of K_6^{EM-AM} and K_{12}^{EM-AM} as described under "Results."

^c Determined by EPR and PRR.

^d Determined by EPR.

^e Determined by PRR.

^f Determined by PRR in competition with Mn^{2+} .

^g Determined from Equations 3–5.

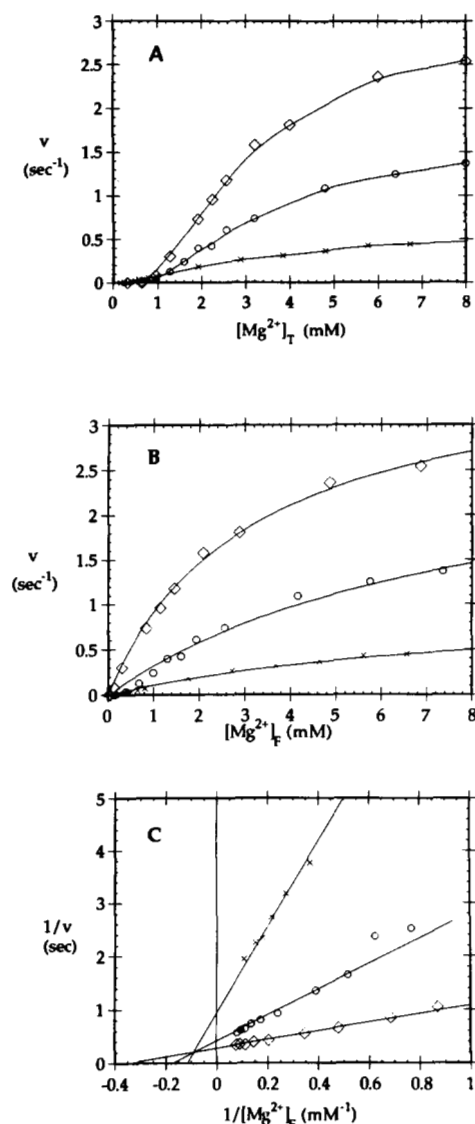


FIG. 3. Mg^{2+} activation of the MutT dGTPase. Panel A, initial velocity of the MutT reaction (mol of dGTP/mol of MutT/s) as a function of total $MgCl_2$ concentration, and at dGTP concentrations of 1,140 μ M (\diamond), 640 μ M (\circ), and 112 μ M (\times). Panel B, initial velocity of MutT reaction as a function of free Mg^{2+} concentration and at Mg^{2+} -dGTP concentrations of 1,140 μ M (\diamond), 640 μ M (\circ), and 112 μ M (\times). Also present was 50 mM Tris-Cl, pH 7.5, and 33 nM MutT. Panel C, double-reciprocal plot of the data in panel B. Data in panels B and C are fit to the equation $v = k_{cat}[Mg^{2+}]_F / (K_m^{Mg^{2+}} + [Mg^{2+}]_F)$.

constant free metal. At 1 mM free Mn^{2+} Mn^{2+} -AMPCPP is a linear competitive inhibitor (Fig. 4A) with a K_i of 42 ± 10 μ M, about 4-fold weaker than the $K_{m(app)}$ for Mn^{2+} -dGTP. Fig. 4B shows the K_i of Mg^{2+} -AMPCPP versus Mg^{2+} -dGTP at 8 mM free $[Mg^{2+}]$. Mg^{2+} -AMPCPP is also a linear competitive inhibitor with a K_i of $2,400 \pm 500$ μ M. Again, this is 4.8-fold weaker than the $K_{m(app)}$ for Mg^{2+} -dGTP at this level of $[Mg^{2+}]_F$. A comparison of K_i values (Table I) reveals Mn^{2+} -AMPCPP to be a 57-fold more potent inhibitor than Mg^{2+} -AMPCPP.

Binding Studies

Separate thermodynamic experiments were done to analyze metal and nucleotide binding to MutT, since kinetic data alone can often be explained by more than one mechanism. Mn^{2+} was used as a paramagnetic probe since the kinetics suggest a similar mode of activation by Mn^{2+} . Both EPR and NMR spectroscopy were used to evaluate the thermodynamics of metal and

AMPCPP binding to MutT. The measured dissociation constants are defined in Table II.

Binary Complexes—Fig. 5A shows the results of a titration of $MnCl_2$ from 117 to 1053 μ M in the presence of 379 μ M MutT, measuring the free Mn^{2+} by EPR. The Scatchard plot in Fig. 5A shows that MutT protein binds Mn^{2+} at 0.91 ± 0.10 sites with a K_2^{E-M} of 163 ± 30 μ M. The enhancement factor (ϵ^*) was measured at each point in this titration and corrected for the free Mn^{2+} by the EPR data according to Equation 2. The resulting ϵ_b^{EM} value was 17 ± 4 . When this ϵ_b value was used to recalculate $[Mn^{2+}]_F/[Mn^{2+}]_T$ from the observed enhancement, ϵ^* , at each point in the titration, a Scatchard analysis yielded a stoichiometry of 0.74 ± 0.20 and a K_2^{E-M} of 100 ± 50 μ M in reasonable agreement with the EPR data. The average value of K_2^{E-M} (130 ± 40 μ M) is comparable to the kinetically determined activator constant of Mn^{2+} , $K_a^{Mn} = 230 \pm 72$ μ M (Table I).

The substrate analog AMPCPP was found, both by EPR and by $1/T_1$ of water protons, to bind one Mn^{2+} ion with a dissociation constant (K_3) of 12 ± 5 μ M and an enhancement factor (ϵ_b^{AM}) of 1.8 ± 0.5 . These values are very similar to those previously found for Mn^{2+} -ATP (Mildvan and Cohn, 1966).

In the absence of metal ions, nucleotides bind very weakly to MutT. Thus, no interaction between MutT and dGTP was detected using a nitrocellulose filter binding assay at 2.5 mM levels of nucleotide and 600 μ M enzyme, indicating a dissociation constant exceeding 2.5 mM. ¹⁵N-enriched MutT was then titrated with AMPCPP and the changes in chemical shifts of selected side chain and backbone NH and ¹⁵N resonances were monitored in consecutive HSQC spectra (not shown). As AMPCPP bound to MutT, changes in NH and ¹⁵N chemical shifts occurred in nine backbone and one side chain amide groups, the largest change (0.08 ppm in the proton dimension and 0.22 ppm in the ¹⁵N dimension) occurring in the side chain ¹⁵NH resonances of a Gln or Asn residue. These changes in chemical shift, as a function of AMPCPP concentration, were well fit by a hyperbolic titration curve (not shown), yielding a dissociation constant (K_1) of $5,100 \pm 600$ μ M under the conditions given under "Methods." Similar analyses of changes in chemical shifts of backbone ¹⁵NH resonances yielded the same K_1 value, within experimental error.

Ternary and Quaternary Complexes—Fig. 5B shows a Scatchard plot of the combined results of two $MnCl_2$ titrations in the presence of either 20 μ M AMPCPP with 20 μ M MutT or 40 μ M MutT with 40 μ M AMPCPP. At concentrations of Mn^{2+} below 16 μ M, and at site occupancies < 0.6 , the level of free Mn^{2+} could not be determined accurately by EPR because of the tightness of the metal binding. Hence the dissociation constant of the tighter site could not be evaluated by this experiment. The Scatchard plot shows that a total of 2.0 ± 0.1 Mn^{2+} are bound to the MutT-AMPCPP complex with a dissociation constant of 16.2 ± 2.0 μ M for the weaker of the two sites, consistent with the dual divalent cation requirement found by the kinetic analysis. Moreover, this dissociation constant agrees with the kinetically determined $K_m^{Mn^{2+}}$ of 26 ± 10 μ M obtained with Mn^{2+} -dGTP as substrate (Table I), suggesting it to be K_{11} (Table II). The presence of the nucleotide AMPCPP thus increases the stoichiometry of Mn^{2+} binding to MutT to 2.0 and raises the affinity of MutT for Mn^{2+} by at least 8-fold (Fig. 5B and Tables I and II).

The enhancement factor (ϵ^*) of water protons was determined at each point in the titration of MutT-AMPCPP with Mn^{2+} and corrected for free $[Mn^{2+}]$ as described above. A plot of the enhancement factor due to bound Mn^{2+} (ϵ_b) against Mn^{2+} site occupancy (Fig. 5C) shows a linear increase with occupancy. The average enhancement for the quaternary complex $E(Mn^{2+})_2AMPCPP$ (ϵ_q) is estimated as 7.1 ± 1.0 by linear extrapolation to a site occupancy of 2.0. The average enhancement (ϵ_t) of either possible ternary complex, $E_{AMPCPP}^{Mn^{2+}}$ or

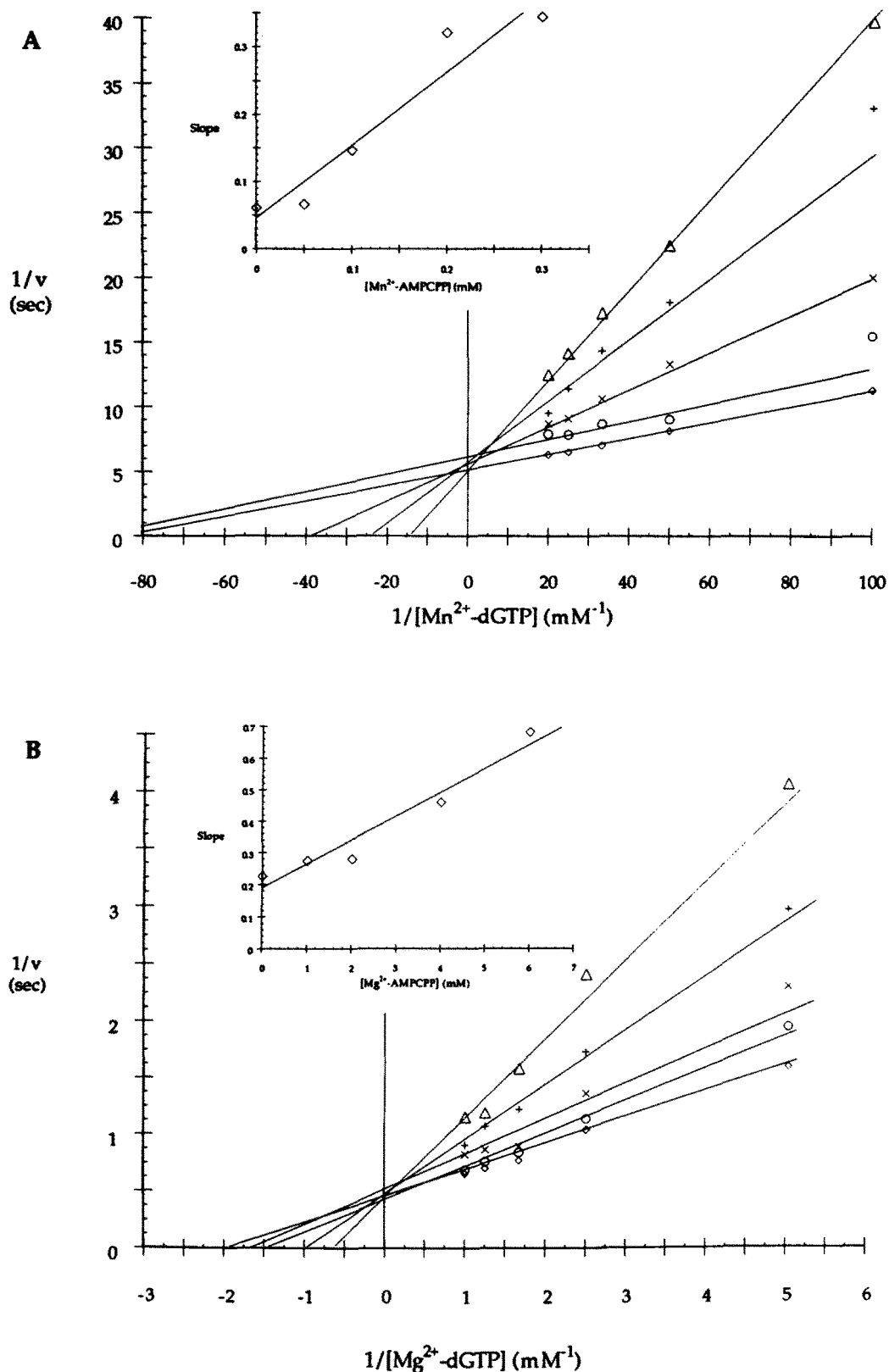


FIG. 4. Inhibition of MutT dGTPase by AMPCPP. Panel A, double-reciprocal plot of initial velocity against Mn^{2+} -dGTP concentration at 1 mM free Mn^{2+} and 0.0 (\diamond), 50 (\circ), 100 (\times), 200 ($+$), and 300 μM (Δ) Mn^{2+} -AMPCPP. The inset shows the secondary plot of the slope versus $[Mn^{2+}\text{-AMPCPP}]$. Also present was 50 mM Tris-Cl, pH 7.5. Panel B, double-reciprocal plot of initial velocity against Mg^{2+} -dGTP concentration at 8 mM free Mg^{2+} and 0.0 (\diamond), 1.0 (\circ), 2.0 (\times), 4.0 ($+$), and 6.0 mM (Δ) Mg^{2+} -AMPCPP. The inset shows the secondary plot of slope versus $[Mg^{2+}\text{-AMPCPP}]$. In panels A and B the lines were computed using weighted least squares analysis. In both insets unweighted linear least squares analyses were used.

TABLE II
Dissociation Constants of Mn^{2+} , Mg^{2+} , and AMPCPP complexes of MutT, and enhancement factors of Mn^{2+} complexes

Parameter	Definition	With Mn^{2+}	With Mg^{2+}
		μM	μM
K_1	(E)(A)/(EA)	$5,100 \pm 600$	$5,100 \pm 600$
K_2	(M)(E)/(EM)	130 ± 40	$7,500 \pm 1,200$
K_3	(A)(M)/(AM)	12 ± 5	50 ± 20
K_4	(EM)(A)/(EMA)	636 ± 224	630 ± 140
K_5	(EM)(A)/(EAM)	12.3 ± 6.6	16 ± 8
K_6	(EM)(AM)/(EMAM)	16.4 ± 4.2	284 ± 220
K_7	(EA)(M)/(EAM)	0.32 ± 0.15	23 ± 11
K_8	(E)(AM)/(EMA)	$6,900 \pm 3,100$	$95,000 \pm 41,000$
K_9	(EMA)(M)/(EMAM)	0.31 ± 0.19	22 ± 14
K_{10}	(M)(EA)/(EMA)	16.2 ± 2.0	932 ± 100
K_{11}	(M)(EAM)/(EMAM)	16.2 ± 2.0	932 ± 100
K_{12}	(E)(AM)/(EAM)	135 ± 30	$2,400 \pm 1,500$
ϵ_b^{AM}	$\epsilon(Mn^{2+} \cdot AMPCPP)$	1.8 ± 0.5	
ϵ_b^{EM}	$\epsilon(E \cdot Mn^{2+})$	17 ± 4	
ϵ_t	$\epsilon(E \cdot AMPCPP \cdot Mn^{2+})$	4.7 ± 0.45	
ϵ_q	$\epsilon(E \cdot Mn^{2+} \cdot AMPCPP \cdot Mn^{2+})$	8.7 ± 1.4	

$E_{AMPCPP \cdot Mn^{2+}}$, is approximated as 3.1 ± 1.0 by linear extrapolation of ϵ_b to zero site occupancy (Fig. 5C) (Armstrong *et al.*, 1979).

The values for ϵ_t and ϵ_q thus obtained are initial estimates since AMPCPP is not saturating. These values were refined using computer analysis of titrations of enzyme and Mn^{2+} with AMPCPP, measuring the enhancement ϵ^* of water protons. Four such titrations (Fig. 6) show the dependence of ϵ^* on [AMPCPP] at several concentrations of total Mn^{2+} . The observed decrease in enhancement upon AMPCPP binding is qualitatively indicative of the formation of a metal-bridge complex. An alternative hypothesis, that the observed decrease in enhancement is caused by the simple removal of the enzyme-bound metal by the nucleotide, is unlikely since under the experimental conditions, all of AMPCPP was in the form $Mn^{2+} \cdot AMPCPP$, and AMPCPP can bind only one metal tightly. The titrations of Fig. 6 were fit to Equation 6 by computer analysis, taking into account all 12 of the dissociation constants as defined in Table II and their relationships (Equations 3–5). K_{10} and K_{11} , which describe the binding of metal to the enzyme site of MutT-AMPCPP and of MutT-AMPCPP- Mn^{2+} , respectively, were both assumed to be $16.2 \pm 2.0 \mu M$ as found in Fig. 5B.² Initial estimates of ϵ_t and ϵ_q were determined as shown in Fig. 5C, and an initial estimate for K_6 was made from the K_i of AMPCPP in the Mn^{2+} -activated reaction. The fits were refined by varying K_1 , K_2 , K_3 , K_{10} , K_{11} , ϵ_b^{AM} and ϵ_b^{EM} within their experimental errors. The results of the best fits, together with the experimental data from four typical titrations, are shown in Fig. 6, and the resulting constants are given in Table II.

To compare the dissociation constant of $Mn^{2+} \cdot AMPCPP$ with the kinetically determined K_i of $Mn^{2+} \cdot AMPCPP$, one must take into account the fact that under the conditions of the kinetic experiment, the inhibitor, $Mn^{2+} \cdot AMPCPP$, binds to both free enzyme (K_{12}) and to the enzyme- Mn^{2+} complex (K_6). From the measured value of the dissociation constant of the binary enzyme- Mn^{2+} complex ($K_2 = 130 \mu M$), at 1 mM free Mn^{2+} and 33 nM MutT, 11% of the enzyme is free, and 89% is in a binary enzyme- Mn^{2+} complex. A correspondingly weighted average of K_{12} (135 μM) and K_6 (16.4 μM) for $Mn^{2+} \cdot AMPCPP$ binding to free MutT and to MutT- Mn^{2+} , respectively, is $29 \pm 7 \mu M$, which agrees, within error, with the K_i of $Mn^{2+} \cdot AMPCPP$ of $42 \pm 10 \mu M$ (Table I).

² Alternative assumptions that the 16.2 μM site represents the dissociation constants of Mn^{2+} from the enzyme-bound nucleotide (K_7 , K_9) or that the dissociation constants K_7 , K_9 , K_{10} , and K_{11} were all equal to 16.2 μM led to poor fits to the titration data of Fig. 6 and to unreasonable values for K_{12} and K_6 , the dissociation constants of $Mn^{2+} \cdot AMPCPP$ from MutT and MutT- Mn^{2+} , respectively.

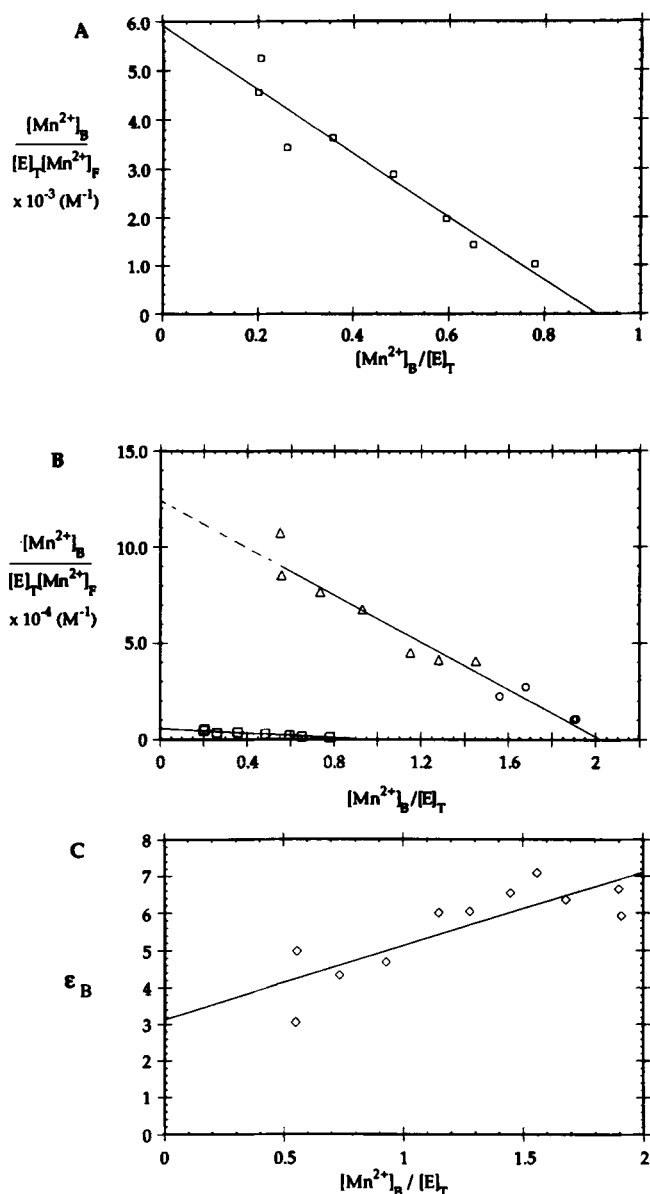


FIG. 5. Mn^{2+} binding by MutT and Mut-AMPCPP. Panel A, Scatchard plot of Mn^{2+} titrated from 117 to 1,053 μM with 379 μM MutT. Also present was 50 mM Tris-Cl, pH 7.5. Panel B, Scatchard plot showing the data from panel A (\square) for comparison, and the data from two titrations of Mn^{2+} (16–129 μM $MnCl_2$) with 20 μM MutT and 20 μM AMPCPP (Δ) or 40 μM MutT and 40 μM AMPCPP (\circ). Also present was 50 mM Tris-Cl, pH 7.5. The broken line indicates that adequate data could not be obtained in the region of low site occupancy. Panel C, plot of the enhancement of $1/T_1$ of water protons caused by bound Mn^{2+} (ϵ_b) as a function of Mn^{2+} site occupancy. Lines in panels A–C are computed using linear least squares analysis.

Mg^{2+} Binding—The dissociation constants, K_2 , K_7 , K_9 , K_{10} , and K_{11} for Mg^{2+} were determined by competition with Mn^{2+} (Serpensu *et al.*, 1986) monitoring the appearance of free Mn^{2+} by EPR (not shown) and by the decrease in ϵ^* resulting from the displacement of bound Mn^{2+} (Fig. 7). Fig. 7A shows the displacement of Mn^{2+} by Mg^{2+} from the binary MutT- Mn^{2+} complex. This experiment was repeated at three other concentrations of Mn^{2+} ranging from 34.3 to 102.8 μM . Consistent with competition between Mn^{2+} and Mg^{2+} for a single binding site, complete displacement of Mn^{2+} was detected by EPR, and a self-consistent $K_2^{Mg^{2+} \cdot MutT}$ was calculated to be 7.5 ± 1.2 mM. This value is comparable to the activator constant of Mg^{2+} ($K_a = 14.6 \pm 7$ mM) determined kinetically (Table I). In the presence of

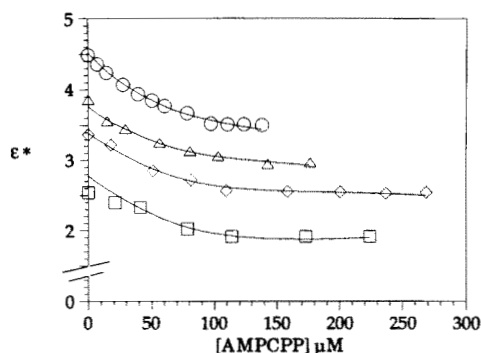


FIG. 6. Titrations of the MutT·Mn²⁺ complex with AMPCPP. A solution containing AMPCPP and the other components of the titration, to avoid dilution, was added stepwise to solutions containing 80 μM MutT and MnCl₂ concentrations of 294 μM (○), 306 μM (△), 382 μM (◇), and 574 μM (□). Also present was 50 mM Tris-Cl, pH 7.5. The curves represent ε* values computed using the parameters given in Table II.

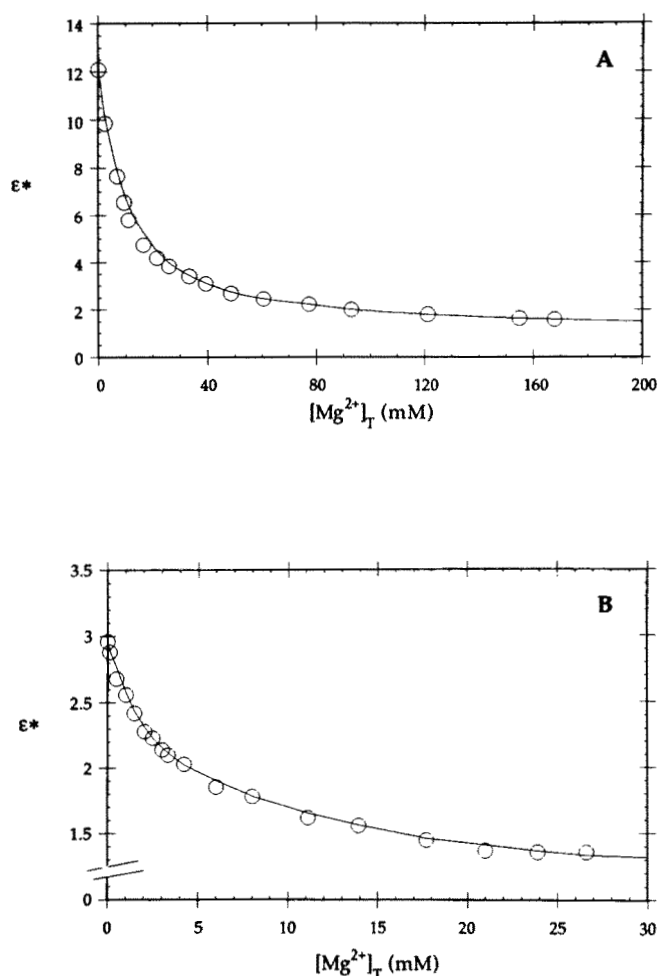


FIG. 7. Displacement of Mn²⁺ from MutT·Mn²⁺ complexes by Mg²⁺. Panel A, titration of 214 μM MutT and 68 μM MnCl₂ with a solution containing MgCl₂ and the other components of the titration, to avoid dilution. Panel B, titration of 20 μM MutT, 43 μM AMPCPP, and 91.4 μM MnCl₂ with a solution containing MgCl₂ and other components of the titration. Also present was 50 mM Tris-Cl, pH 7.5. Dissociation constants for Mg²⁺ were determined by the method of Serspersu *et al.* (1986) and are given in Table II.

AMPCPP (Fig. 7B) Mg²⁺ also displaced bound Mn²⁺. Four such titrations at Mn²⁺ concentrations ranging from 68 μM to 114 μM reveal simple competition by the above criteria and yield average values of K_{10} and K_{11} of 0.9 ± 0.1 mM which agree with the kinetically determined $K_m^{Mg^{2+}}$ of 1.7 ± 0.7 mM (Table I). These

titrations also permitted the evaluation of $K_7^{E\text{-AMPCPP}\cdot Mg^{2+}}$ and $K_5^{E\text{-Mg}^{2+}\cdot AMPCPP\cdot Mg^{2+}}$ by competition with Mn²⁺ at the corresponding nucleotide site. $K_1^{E\text{-AMPCPP}}$ was measured independently by NMR, as described above. Since $K_3^{Mn^{2+}\cdot AMPCPP}$ was shown above to be equal to $K_3^{Mn^{2+}\cdot ATP}$ (Mildvan and Cohn, 1966), it was reasonably assumed that $K_3^{Mg^{2+}\cdot AMPCPP}$ was equal to $K_3^{Mg^{2+}\cdot ATP}$ (Dawson *et al.*, 1986). With $K_1, K_2, K_3, K_7, K_9, K_{10}$, and K_{11} in hand, the remaining dissociation constants for the MutT·Mg²⁺·AMPCPP·Mg²⁺ complex could be calculated from Equations 3–5 and are listed in Table II.

Substrate Properties of Co³⁺(NH₃)₄ATP—Fig. 8A shows the substitution inert β,γ-bidentate complex Co³⁺(NH₃)₄ATP to be a substrate for MutT, as monitored by the appearance of AMP, only in the presence of added Mg²⁺ (20 mM) or Mn²⁺ (2 mM) (not shown), confirming that a second metal, in addition to the one complexed by the nucleotide, is essential for catalysis. After prolonged incubation for 6 h at 23 °C, approximately 50% of the racemic mixture of Co³⁺(NH₃)₄ATP is hydrolyzed as shown in Fig. 8A and in five separate experiments. After such prolonged incubation, MutT remains active. Thus, when additional Co³⁺(NH₃)₄ATP is added, half is again hydrolyzed (Fig. 8A). The maximal velocity of hydrolysis of Co³⁺(NH₃)₄ATP by Mg²⁺-activated MutT is 4×10^{-3} s⁻¹. In comparison, the corresponding maximal velocity with Mg²⁺·ATP as substrate is 0.08 s⁻¹ under the same conditions. These kinetic experiments thus indicate that MutT is 5% as active on Co³⁺(NH₃)₄ATP as on Mg²⁺·ATP under otherwise identical conditions, but only on one of the two stereoisomers of the Co³⁺ complex.

Because of chirality at the β-phosphorus, Co³⁺(NH₃)₄ATP as prepared consists of a racemic mixture of the Δ and Λ stereoisomers (Fig. 8B). The CD spectrum of this racemic mixture has both positive and negative ellipticity in the region of absorption by Co³⁺ because of imperfect cancellation of the CD spectra of the two stereoisomers (Fig. 8B) (Granot *et al.*, 1979). Changes in the CD spectrum of the mixture with time are observed in the presence of MutT only when Mg²⁺ (20 mM) is also present (Fig. 8B), confirming the requirement for a second metal ion in addition to the one coordinated by the nucleotide. When both MutT and Mg²⁺ are present, the positive ellipticity disappears with time, indicating the loss of the Λ isomer, and the negative ellipticity of the Δ isomer remains (Fig. 8B). Since the negative ellipticity of the Δ stereoisomer has been established by x-ray crystallography (Merritt *et al.*, 1978), the data of Fig. 8B establish the stereoselectivity of MutT for the Λ stereoisomer of Co³⁺(NH₃)₄ATP.

In a separate experiment, the authentic Δ isomer of Co³⁺(NH₃)₄ATP, prepared by treatment of the racemic mixture with glucose and hexokinase (which also prefers the Λ stereoisomer) and purified, gave a CD spectrum identical to that of the stereoisomer remaining after the MutT reaction. Prolonged incubation of the Δ isomer of Co³⁺(NH₃)₄ATP with a high concentration of MutT (160 μM) and Mg²⁺ (20 mM) showed negligible hydrolysis of the Δ isomer (<6%) after 6 h at 23 °C.

DISCUSSION

Like several other enzymes that catalyze nucleophilic substitution at the electron rich β-phosphorus of NTP, the MutT enzyme requires two divalent cations for catalytic activity. Three lines of evidence support this conclusion. First, additional Mn²⁺ (or Mg²⁺) well beyond that required to saturate dGTP is necessary to activate hydrolysis (Figs. 1–3). Second, although MutT alone binds one Mn²⁺ (or Mg²⁺) per mol of enzyme, the MutT complex of the substrate analog AMPCPP binds two divalent cations, with dissociation constants at the weaker site very similar to those found by kinetic analysis (Fig. 5 and Table I). Third, the Λ stereoisomer of the substitution inert Co³⁺(NH₃)₄ATP complex shows substrate activity with

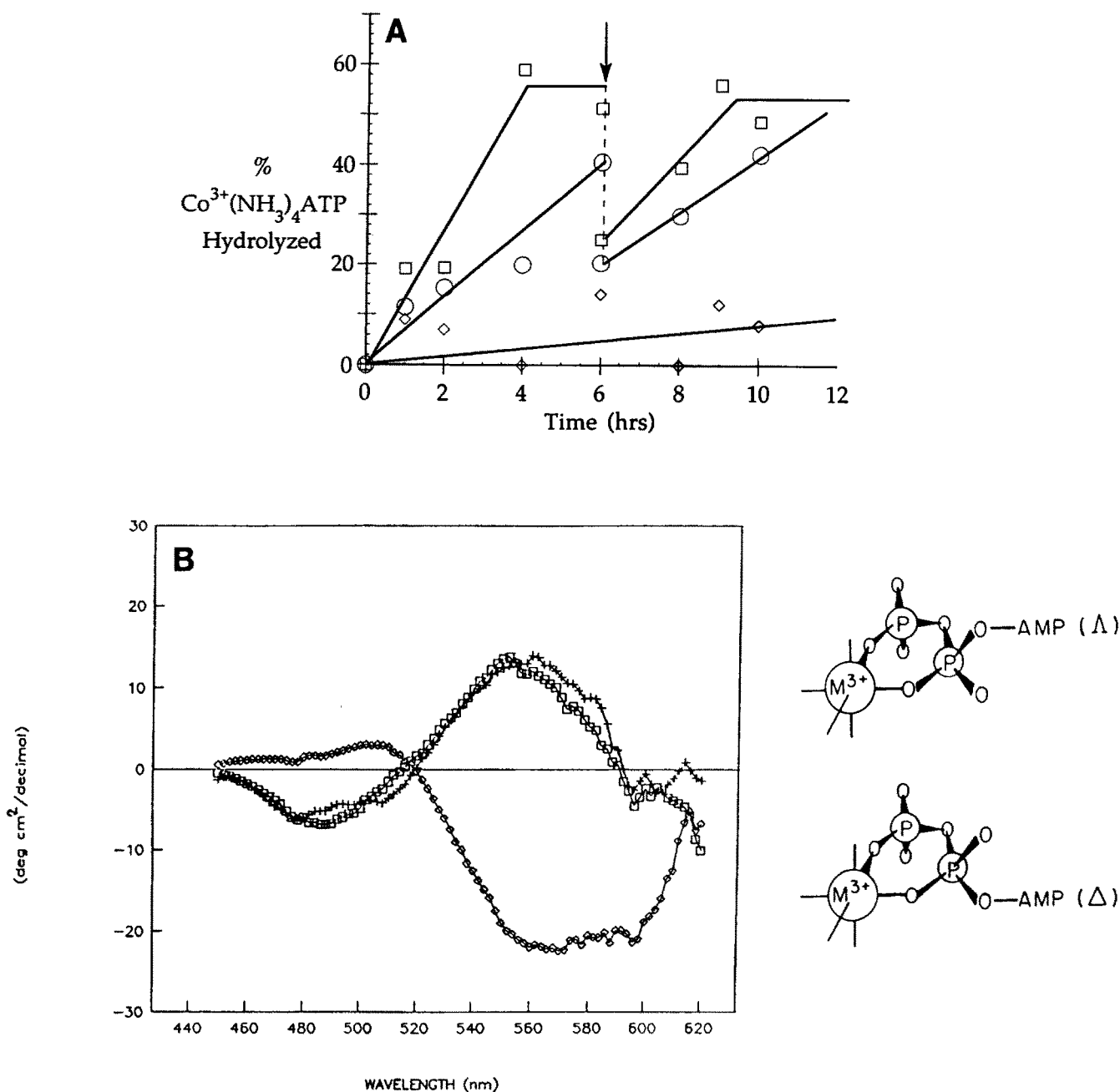


FIG. 8. Hydrolysis of $\text{Co}^{3+}(\text{NH}_3)_4\text{ATP}$ in the presence of MutT. Panel A, percent $\text{Co}^{3+}(\text{NH}_3)_4\text{ATP}$ hydrolyzed as determined by AMP formed in reaction mixtures containing 3.5 mM $\text{Co}^{3+}(\text{NH}_3)_4\text{ATP}$ and 60 μM MutT (\diamond), 30 μM MutT plus 20 mM MgCl_2 (\circ), or 60 μM MutT plus 20 mM MgCl_2 (\square). Also present was 50 mM Tris-Cl, pH 7.5. After 6 h, as indicated by the arrow, the concentration of $\text{Co}^{3+}(\text{NH}_3)_4\text{ATP}$ was doubled to 7.0 mM. Panel B, circular dichroism spectra of 5.0 mM $\text{Co}^{3+}(\text{NH}_3)_4\text{ATP}$ alone (\square), with 37 μM MutT (+), or with 37 μM MutT plus 20 mM MgCl_2 (\diamond) after 6 h at 23 °C in 50 mM Tris-Cl, pH 7.5. Insets show the structures of the Δ isomer, which contributes to the positive ellipticity, and the Δ isomer, which contributes to the negative ellipticity.

MutT, but only in the presence of added Mg^{2+} or Mn^{2+} , establishing that the nucleotide-bound metal alone is not sufficient for catalytic activity (Fig. 8).

The coordination scheme of the active complex is likely to be a metal-bridge complex of the form enzyme· M^{2+} ·NTP· M^{2+} based on five lines of evidence. First, the enzyme· M^{2+} complex binds M^{2+} ·NTP significantly more tightly than does the free enzyme as found by kinetic studies with both Mn^{2+} and Mg^{2+} ($K_m^{\text{M}^{2+}\cdot\text{dGTP}} \ll K_m^{\text{M}^{2+}\cdot\text{dGTP}}$) (Table I) and by direct binding studies with Mn^{2+} ·AMPCPP ($K_6^{\text{EM}\cdot\text{AM}} \ll K_{12}^{\text{EM}\cdot\text{AM}}$) (Table II). Second, binding of M^{2+} ·NTP to the enzyme raises the affinity of the enzyme for M^{2+} as found both by kinetic studies ($K_m^{\text{M}^{2+}} \ll K_a^{\text{M}^{2+}}$) (Table I) and by metal binding studies with both Mn^{2+} and Mg^{2+}

($K_{11}^{\text{EM}\cdot\text{AM}} \ll K_2^{\text{EM}}$) (Table II). Third, changing the divalent cation activator from Mn^{2+} to Mg^{2+} significantly weakens the binding of the metal-nucleotide to the enzyme-metal complex, as detected by kinetic analysis ($K_m^{\text{Mg}^{2+}\cdot\text{dGTP}} \gg K_m^{\text{Mn}^{2+}\cdot\text{dGTP}}$ and $K_7^{\text{Mg}^{2+}\cdot\text{AMPCPP}} \gg K_7^{\text{Mn}^{2+}\cdot\text{AMPCPP}}$) (Table I), and by binding studies ($K_6^{\text{EMg}^{2+}\cdot\text{AMPCPP}\cdot\text{Mg}} \gg K_6^{\text{EMn}^{2+}\cdot\text{AMPCPP}\cdot\text{Mn}^{2+}}$) (Table II), suggesting a direct interaction of the enzyme-bound metal with M^{2+} ·AMP-CPP. Fourth, the paramagnetic effect of enzyme-bound Mn^{2+} on $1/T_1$ of water protons is markedly decreased on binding of AMP-CPP or Mn^{2+} ·AMPCPP. Thus, the 17-fold enhancement factor in the binary enzyme· Mn^{2+} complex decreases to average values of 4.7 in the ternary complex and to 8.7 in the quaternary complex (Table II), indicating decreased access of water protons

to enzyme-bound Mn^{2+} when AMPCPP or Mn^{2+} -AMPCPP is bound. Fifth, although the substitution inert β,γ -bidentate $Co^{3+}(NH_3)_4ATP$ is a relatively poor substrate, its activity in the presence of Mg^{2+} indicates that the nucleotide-bound metal is likely to be β - and γ -coordinated and need not be directly coordinated to the enzyme.³ Clearly, a major catalytic role of the nucleotide-bound metal ion is to activate the β -phosphoryl group for nucleophilic attack by electron withdrawal and, possibly, by transition state stabilization.

Four possible catalytic roles for the enzyme-bound divalent cation in the active, quaternary $MutT \cdot M^{2+} \cdot dGTP \cdot M^{2+}$ complex may be considered. First, like the nucleotide-bound metal ion, the bridging divalent cation may also coordinate the β -phosphoryl group, further activating this electron-rich position for nucleophilic attack. Second, by coordinating the α -phosphoryl group of dGTP, the bridging metal ion may facilitate the departure of the leaving group, dGMP. Third, the enzyme-bound divalent cation may coordinate and activate the other substrate, the attacking water molecule. Fourth, the bridging metal ion may adjust the protein conformation, bringing appropriate catalytic groups into contact with both substrates. NMR studies of the structure of the quaternary complex formed by phosphoribosyl pyrophosphate synthetase revealed the enzyme-bound Mn^{2+} to form a second sphere enzyme- $Mn^{2+}(H_2O) \cdot ATPCo^{3+}(NH_3)_4$ complex (Granot *et al.*, 1980). With the enzymes phosphoenolpyruvate synthase and pyruvate-orthophosphate dikinase, NMR and EPR studies indicate a role of the enzyme-bound metal as coordinating the nonnucleotide substrate, pyruvate (Berman and Cohn, 1970; Kofron *et al.*, 1988). Proof of a $MutT \cdot M^{2+} \cdot NTP \cdot M^{2+}$ complex and elucidation of the precise roles of the two metal ions will require detailed structural studies by NMR, which are in progress (Abeygunawardana *et al.*, 1993; Weber *et al.*, 1993).

Acknowledgments—We are grateful to C. Abeygunawardana for the NMR instrumentation, to R. L. Koder for help in synthesizing and in characterizing the $Co^{3+}(NH_3)_4ATP$ complex, to Damian Hammontree for help with computation, to Linda C. Bullions for valuable discussions, to John Ruble for technical assistance, and to Peggy Ford for secretarial assistance.

³ With the more active Mn^{2+} and Mg^{2+} -NTP complexes, the nucleotide-bound metal may also receive ligands from the enzyme as suggested by the increases in $K_s^{M^{2+} \cdot dGTP}$ (Table I) and in $K_{12}^{2 \cdot AM}$ (Table II) on changing the divalent cation from Mn^{2+} to Mg^{2+} .

REFERENCES

- Abeygunawardana, C., Weber, D. J., Frick, D. N., Bessman, M. J., and Mildvan, A. S. (1993) *Abstracts of the Experimental NMR Conference, St. Louis, MO, March 14–18, 1993*, Poster 43, p. 94
- Adams, H. (1965) in *Methods in Enzymatic Analysis* (Bergmeyer, H. U., ed) pp. 575–577, Academic Press, New York
- Akiyama, M., Maki, H., Sekiguchi, M., and Horiuchi, T. (1989) *Proc. Natl. Acad. Sci. U. S. A.* **86**, 3949–3952
- Armstrong, R. N., Kondo, H., Granot, J., Kaiser, E. T., and Mildvan, A. S. (1979) *Biochemistry* **18**, 1230–1238
- Berman, K., and Cohn, M. (1970) *J. Biol. Chem.* **245**, 5309–5318
- Bhatnagar, S. K., and Bessman, M. J. (1988) *J. Biol. Chem.* **263**, 8953–8957
- Bhatnagar, S. K., Bullions, L. C., Lew, G., and Bessman, M. J. (1990) *J. Bacteriol.* **172**, 2802–2803
- Bhatnagar, S. K., Bullions, L. C., and Bessman, M. J. (1991) *J. Biol. Chem.* **266**, 9050–9054
- Bullions, L. C. (1993) *Studies on the MutT Enzyme from E. coli and S. pneumoniae*. Ph.D. thesis, The Johns Hopkins University, Baltimore
- Carr, H. Y., and Purcell, E. M. (1954) *Phys. Rev.* **94**, 630–638
- Cleland, W. W., and Mildvan, A. S. (1979) in *Advances in Inorganic Biochemistry* (Eichorn, G. L., and Marzilli, L. G., eds) pp. 163–191, Elsevier, North Holland, Amsterdam
- Cohn, M., and Townsend, J. (1954) *Nature* **173**, 1090–1091
- Cornelius, R. D., and Cleland, W. W. (1978) *Biochemistry* **17**, 3279–3286
- Cornelius, R. D., Hart, P. A., and Cleland, W. W. (1988) *Inorg. Chem.* **16**, 2799–2805
- Dawson, R. M. C., Elliot, D. C., Elliot, W. H., and Jones, K. M. (1986) *Data for Biochemical Research*, pp. 413–415, Oxford University Press, New York
- Dixon, M., and Webb, E. C. (1964) *Enzymes*, pp. 438–439, Academic Press, London
- Fowler, R. G., Amutan, M. V., and Isbell, R. J. (1992) *Mutat. Res.* **284**, 307–319
- Frick, D. N., Weber, D. J., Bessman, M. J., and Mildvan, A. S. (1993) *FASEB J.* **7**, A1064 (abstr.)
- Granot, J., Mildvan, A. S., Brown, E. M., Kondo, H., Bramson, N., and Kaiser, E. T. (1979) *FEBS Lett.* **103**, 265–269
- Granot, J., Gibson, K. J., Switzer, R. L., and Mildvan, A. S. (1980) *J. Biol. Chem.* **255**, 10931–10937
- Kay, L. E., Ikura, M., Tschudin, R., and Bax, A. (1990) *J. Magn. Reson.* **89**, 496–514
- Kaziro, Y. (1959) *J. Biochem.* **46**, 1523–1539
- Kofron, J. L., Ash, D. E., and Reed, G. H. (1988) *Biochemistry* **27**, 4781–4787
- Li, T. M., Mildvan, A. S., and Switzer, R. L. (1978) *J. Biol. Chem.* **253**, 3918–3923
- Marion, D., Ikura, M., Tschudin, R., and Bax, A. (1989) *J. Magn. Reson.* **85**, 393–399
- Merrit, E. A., Sundaralingam, M., Cornelius, R. D., and Cleland, W. W. (1978) *Biochemistry* **17**, 3274–3279
- Michaels, G., Milner, Y., Moskovitz, B. R., and Wood, H. G. (1978) *J. Biol. Chem.* **253**, 7656–7661
- Mildvan, A. S. (1970) in *The Enzymes* (Boyer, P. D., ed) vol. 2, pp. 446–536, Academic Press, New York
- Mildvan, A. S., and Cohn, M. (1963) *Biochemistry* **2**, 910–919
- Mildvan, A. S., and Cohn, M. (1966) *J. Biol. Chem.* **241**, 1178–1193
- Mildvan, A. S., and Engle, J. L. (1972) *Methods Enzymol.* **26C**, 654–683
- Mo, J.-Y., Maki, H., and Sekiguchi, M. (1992) *Proc. Natl. Acad. Sci. U. S. A.* **89**, 11021–11025
- Serpensu, E. H., Shortle, D., and Mildvan, A. S. (1986) *Biochemistry* **25**, 68–77
- Shiota, T., Baugh, C. M., Jackson, R., and Dillard, R. (1969) *Biochemistry* **8**, 5022–5028
- Switzer, R. L. (1971) *J. Biol. Chem.* **246**, 2447–2458
- Sy, J., and Lipmann, F. (1973) *Proc. Natl. Acad. Sci. U. S. A.* **70**, 306–309
- Treffers, H. P., Spinelli, V., and Belser, N. O. (1954) *Proc. Natl. Acad. Sci. U. S. A.* **42**, 1064–1071
- Weber, D. J., Bhatnagar, S. K., Bullions, L. C., Bessman, M. J., and Mildvan, A. S. (1992) *J. Biol. Chem.* **267**, 16939–16942
- Weber, D. J., Abeygunawardana, C., Frick, D. N., Bessman, M., and Mildvan, A. S. (1993) *FASEB J.* **7**, A1289 (abstr.)
- Yanofsky, C., Cox, E. C., and Horn, V. (1966) *Proc. Natl. Acad. Sci. U. S. A.* **55**, 274–281